

Performance Evaluation Experiment of High Power Transponder

Kazuyoshi KAWASAKI

Experimental telecommunications equipment of the Ka and S band was installed in Engineering Test Satellite VIII (ETS-VIII: KIKU No.8) launched in December, 2006. To investigate the secular distortion of this experimental telecommunications equipment, five times performance evaluation experiment was done.

This experiment result represents an evaluation for the secular distortion of the equipment equipped to the satellite on the orbit, and it becomes a help in designing and production of the equipment installed to the satellite in the future.

1 Introduction

The Engineering Test Satellite VIII (hereinafter ETS-VIII) was developed for the purpose of technology development and demonstration required for satellite communications with onboard large-deployable antennae and with small mobile stations that use the antennae. It was launched by an H-IIA rocket No.11 on 18 December 2006.

This satellite carries Ka-band (30 GHz/20 GHz band)

frequency communication equipment to be used as a feeder link between the ground base station and the satellite, and S-band (2.6 GHz/2.5 GHz band) equipment to be used as a service link between the small mobile station and the satellite, which enables us to conduct various types of experiments by changing the connection path of the communication equipment. Also, there are choices for a relay system, either the regenerative mode, that relays signals through a switch, or the bent-pipe mode

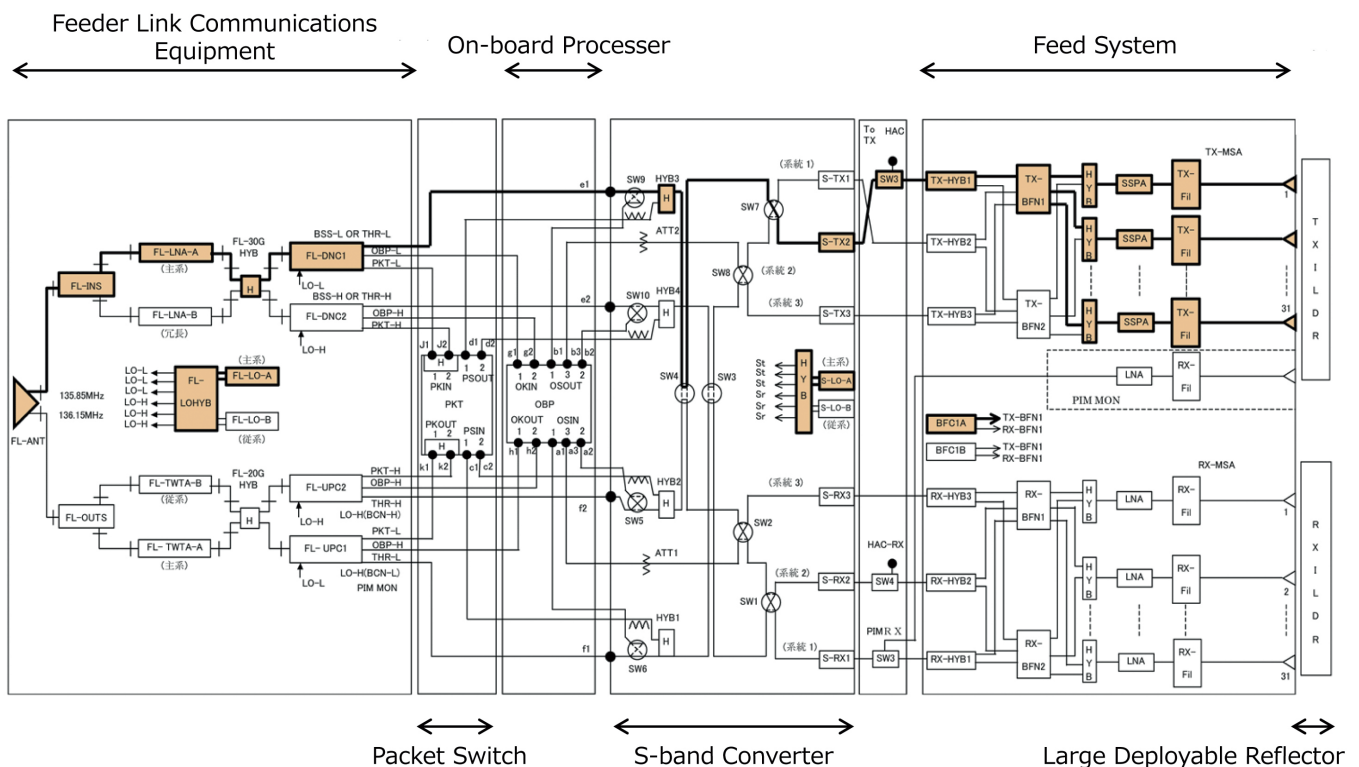


Fig. 1 Composition of transponders

in which signals are relayed without going through the switch and thus without being processed.

In this paper, the author will give an outline of the initial performance evaluation experiment and the regular performance evaluation experiment, and the evaluation results concerning performance and functions of the transponder based on the data obtained from those experiments.

2 An outline of high power transponders^{[1]-[3]}

The high power transponder is composed of the feeder link communications equipment (FLCE), on-board packet switch (PKT), on-board processor (OBP), S-band frequency converter (SCNE), large deployable antenna feed (LDAF) and large deployable antenna reflector (LDR). The composition of the transponder is shown in Fig. 1, the outline of each transponder subsystem in Table 1 and the main specifications of the transponder in Table 2.

FLCE has functions that, after amplifying the received signal of 30 GHz band by a low-noise amplifier (FL-LNA), convert the signal to a 140 MHz band intermediate frequency (IF) signal by a down-converter (FL-DNC) and then output it to a PKT, OBP and S-band frequency converter, and that, after converting an IF signal outputted from a PKT, OBP and S-band frequency converter to a 20 GHz band transmission by an up-converter (FL-UPC) and amplifying the signal power by a

traveling-wave-tube amplifier (FL-TWTA), send the signal to a satellite earth station. FL-TWTA has a transmission output of 8W. FL-UPC and FL-DNC have variable-gain functions. Also, local oscillators for FL-UPC and FL-DNC have frequency-variable functions^[4].

PKT and OBP have functions of exchanging packets and audio signals on satellites.

SCNE is composed of three down-converters (S-RX) that convert the frequency of a received S-band signal to a 140 MHz band IF signal, three up-converters (S-TX) that convert the frequency of an IF signal to an S-band transmission, and 10 IF switches (IF SW) that are to switch paths. S-TX and S-RX have variable-gain functions. Also, local oscillators for S-TX and S-RX have frequency-variable functions^[5].

LDAF is composed of two pairs of beam forming networks (BFN), and 31 solid-state power amplifiers (SSPA), etc. for transmission and reception respectively in order to realize multi-beam phased-array antennae. It mounts 31 SSPAs (eight 20W-class and 23 10W-class ones) and allows for a transmission output of 355W in total^[6]. It is also equipped with 31 cup microstrip antennae (MSA) as feed elements and two LDR of the world-largest size (external form: 19 m × 17 m, antenna aperture diameter: 13 m) both for transmission and reception.

3 An outline of the experiment

In order to obtain the basic performance evaluation

Table 1 Functional overview of transponder subsystems

Mission	Feature Overview
Feeder Link Communications Equipment (FLCE)	Transmit and Receive for Ka-band Signals Frequency Conversion for Ka-band Signals
On-board Packet Switch (PKT)	Function of Exchanging Packet Signals
On-board Processor (OBP)	Function of Exchanging Audio Signals
S-band Converter (SCNE)	Frequency Conversion for S-band Signals Switch Paths
Large Deployable Antenna Feed (LDAF)	Transmit and Receive for S-band Signals
Large Deployable Antenna Reflector (LDR)	Antenna Reflector (Both for Tx and Rx)

Table 2 Specifications of transponders

	Feeder Link	Service Link
RF	30.6 GHz band (Uplink) 20.8 GHz band (Downlink)	2.6 GHz band (Uplink) 2.5 GHz band (Downlink)
IF	140 MHz band	
Polarization	Right-hand Circular Polarization (Uplink) Left-hand Circular Polarization (Downlink)	Left-hand Circular Polarization
Antenna	0.8m Offset Parabolic Antenna	1.0m Parabolic Antenna (HAC) (Uplink) Large Deployable Antenna (Downlink)
Feeding System		Active Phased Array with 31 Feeding Elements
Number of Beams		3 beams (max)

data of communication equipment for Ka-band (30 GHz/20 GHz band) and S-band (2.6 GHz/2.5 GHz band) as a performance evaluation experiment of transponders, we regularly measured the input-output, amplitude-frequency, spurious and frequent-variable characteristics of each communication equipment, and evaluated the equipment's performance and secular change based on the obtained data.

The initial performance evaluation experiment was conducted in February 2007 immediately after the satellite's launch, which was followed by the 1st regular performance evaluation experiment in September 2008, the 2nd in January 2010, the 3rd in January 2011, and the 4th in April 2012.

In addition, as for the low noise amplifier (LNA) for S-band reception, we have been unable to conduct the experiment using this equipment since a failure occurred to the power system which has not been remedied. Consequently, we are conducting the experiment using the S-band's RF section of the high accuracy clock (HAC) as an alternative for this equipment^[7].

4 Composition of the experiment system

We used the Ka-band feeder-link earth station and the S-band earth station of the Kashima Space Technology Center as earth stations, and the continuous wave (CW) as a signal for measurement.

The path within a transponder (hereinafter, relay link) was configured using 10 IF switches (IF SW 1-10) of SCNE as shown in Fig. 1. Also, we used the SW2, an RF switch of a mission integrator that is located on the output side of the S-band up-converter (S-TX2), for switching between the LDAF that was used for S-band transmission and the S-band transmitter of the HAC equipment. For S-band reception, we used the S-band receiver of the HAC equipment since the large deployable antenna was not available due to the trouble with the LNA. For switching paths, we used the SW4, an RF switch of a mission integrator, which is located on the input side of the S-band down-converter (S-RX2).

4.1 Relay link

We used the bent-pipe mode as a relay method to be used for the experiment and the following five routes for relay links.

4.1.1 Cross link using a feeder link

The cross link using a feeder link (FL-CRS) that uses

the Ka-band feeder link for both the uplink (a link from the ground towards the satellite) and the downlink (a link from the satellite towards the ground) was mainly used for the FLCE's performance evaluation experiment. The path of the FL-CRS is shown in Fig. 2.

4.1.2 Forward link

The forward link that uses the Ka-band for the uplink and the S-band large deployable antenna for the downlink was mainly used for the performance evaluation experiment of the S-band transmitter. The path of the forward link is shown in Fig. 3.

4.1.3 Forward link (HAC transmission)

The forward link (HAC transmission) that uses the Ka-band for the uplink and the S-band transmitter of the HAC equipment for the downlink was mainly used for the performance evaluation experiment of the S-band's RF section of the HAC equipment. The path of the forward link (HAC transmission) is shown in Fig. 4.

4.1.4 Cross link using a service link

The cross link using a service link that uses the S-band's RF section of the HAC equipment for the uplink and the S-band large deployable antenna for the downlink was mainly used for the performance evaluation experiment of the S-band receiver. The path of the cross link using a service link is shown in Fig. 5.

4.1.5 Return link

The return link that uses the S-band's RF section of the HAC equipment for the uplink and the Ka-band for the downlink was also mainly used for the performance evaluation experiment of the S-band receiver. The path of the return link is shown in Fig. 6.

5 Experimental details

5.1 Input-output characteristics

We measured the input-output characteristics of respective relay links of the cross link using a feeder link (Fig. 2), forward link (Fig. 3), and forward link (HAC transmission) (Fig. 4).

In the experiment, we transmitted CW to a satellite and measured the strength of signals received from the satellite by a spectrum analyzer. We repeated the measurement while changing the transmission signal level and determined the satellite input/output power by converting the values obtained from the measurement. In addition, we carried out measurement of the forward link of each of 31 SSPAs.

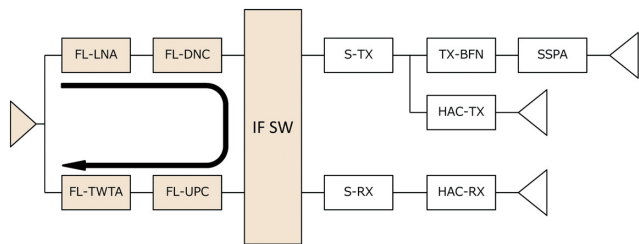


Fig. 2 Cross link using a feeder link

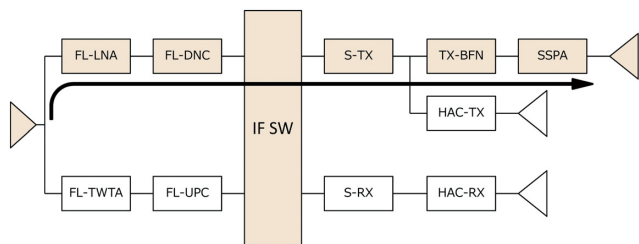


Fig. 3 Forward link

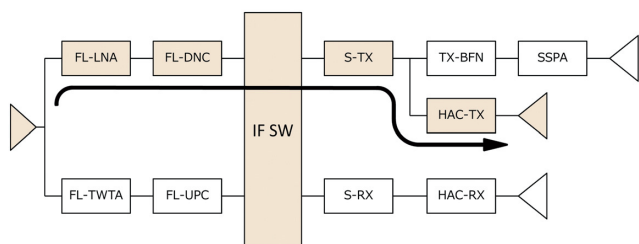


Fig. 4 Forward link (HAC transmission)

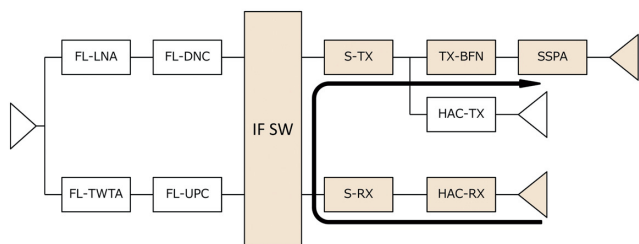


Fig. 5 Cross link using a service link

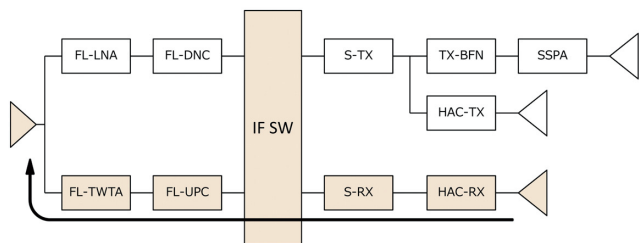


Fig. 6 Return link

5.2 Gain

We measured the gain at each relay link of the cross link using a feeder link (Fig. 2), forward link (Fig. 3),

forward link (HAC transmission) (Fig. 4), cross link using a service link (Fig. 5), and return link (Fig. 6). In the experiment, we measured the strength of returning signals that turned at the satellite transponder, converted the measured values into the satellite input/output power and regarded their difference as the transponder gain.

In addition, we carried out the measurement of the forward link of each of 31 SSPAs and the cross link using a service link of each of three S-band up-converters (S-TX).

5.3 Amplitude-frequency characteristics

We measured the amplitude-frequency characteristics at each relay link of the cross link using a feeder link (Fig. 2), forward link (Fig. 3), forward link (HAC transmission) (Fig. 4), cross link using a service link (Fig. 5), and return link (Fig. 6).

In the experiment, we obtained the values of the receiving spectrum of transponder noise that were calculated 100 times and smoothed on the spectrum analyzer, and evaluated the amplitude-frequency characteristics using those values.

5.4 Spurious characteristics

We measured the spurious characteristics at each relay link of the cross link using a feeder link (Fig. 2), forward link (Fig. 3), forward link (HAC transmission) (Fig. 4), cross link using a service link (Fig. 5), and return link (Fig. 6).

In the experiment, we determined the (in)existence of unnecessary spurious emission by transmitting CW to the satellite and measuring its receiving spectrum.

5.5 Variable-gain characteristics

We measured the variable-gain characteristics at each relay link of the forward link (Fig. 3) and return link (Fig. 6).

The transponder of ETS-VIII mounts up-converters (FL-UPC for Ka-band; S-TX for S-band) and down-converters (FL-DNC for Ka-band; S-RX for S-band). Also, each up-converter and down-converter has a variable-gain function (i.e. step attenuator), and can change the gain by sending commands from the ground.

In the experiment, we measured the strength of receiving signals based on different set values using this variable-gain function.

5.6 Frequency-variable characteristics

We measured the frequency-variable characteristics at

each relay link of the cross link using a feeder link (Fig. 2), forward link (Fig. 3), and cross link using a service link (Fig. 5).

The transponder of ETS-VIII mounts local oscillators for the Ka-band and S-band which are used by up-converters and down-converters. The local oscillator is equipped with a function to change the output frequency, which allows us to change the frequencies of the Ka-band and S-band independently.

In the experiment, we measured the receiving frequency in the case of changing the output frequency of local oscillators using this frequency-variable function.

6 Results and evaluation of the experiment^{[8][9]}

6.1 Input-output characteristics

In the following, the Figs. 7, 8, and 9 show the examples of the measurement results in the cases of using the cross link using a feeder link (Fig. 2), a 20W-class SSPA for S-band transmission at the forward link (Fig. 3) and a 10W-class SSPA for S-band transmission at the forward link (Fig. 3), respectively. The horizontal axes represent the input power to LNAs, and the vertical ones the output power of power amplifiers (TWTA for Ka-band, SSPA for S-band).

Figure 7 explains that the input-output characteristics of the cross link using a feeder link (Fig. 2) are linear, and thus that their variations are smaller compared with the result of the initial performance evaluation experiment. However, depending on the year of measurement, certain variations can be seen in the data in terms of the input-output characteristics of the forward link (Fig. 3) in the Figs. 8 and 9. In this regard, since there are smaller variations in the input-output characteristics at the cross link using a feeder link (Fig. 2), it is supposed that the strength of receiving signals changed due to distortion occurred at LDR at certain points in time^[10].

Thus, it is necessary to pay attention to changes in the strength of receiving signals through time when using the large deployable antenna for S-band transmission even if almost no aging degradation has occurred to the input-output characteristics.

6.2 Gain

Figure 10 shows the measurement results of the gain at 31 S-band SSPAs (eight 20W-class and 23 10W-class ones) at the forward link (Fig. 3). The horizontal axis represents

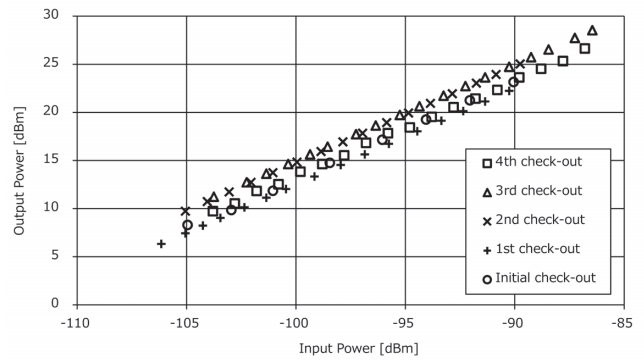


Fig. 7 Input-output characteristics (an example of the cross link using a feeder link)

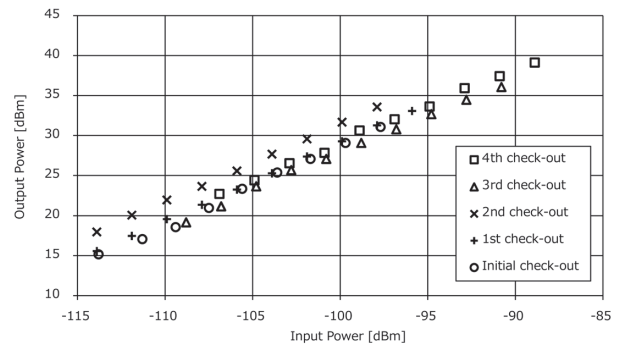


Fig. 8 Input-output characteristics (an example of the 20W-class SSPA at the forward link)

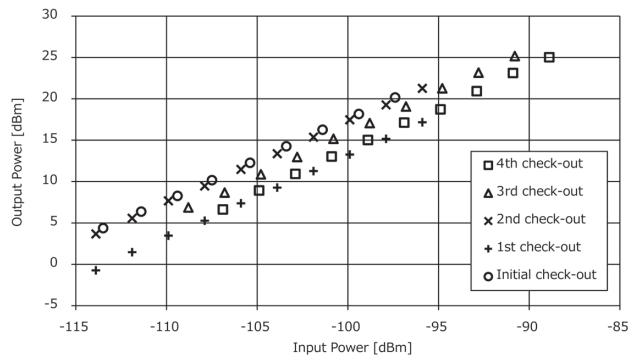


Fig. 9 Input-output characteristics (an example of the 10W-class SSPA at the forward link)

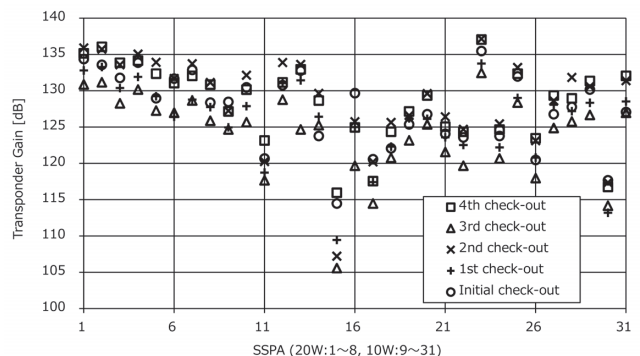


Fig. 10 Transponder gain (forward link)

the 31 SSPAs, while the vertical axis represents the corresponding gain at those SSPAs.

Figure 10 shows that the gain at each SSPA was good as there was no significant gain reduction compared with their initial performance evaluation experiment, which indicates that there was no reduction in the transponder gain due to its aging. Also, it was demonstrated that the transponder has sufficient gain as a transponder and meets the system requirements in terms of the transponder gain.

In addition, there were differences in the gain for different SSPAs not only because of a 3dB difference in the amplification degrees between 20W-class and 10W-class SSPAs, but also because of the array antennae causing differences in the antenna gain at the 31 antenna elements at the Kashima Space Technology Center in Kashima City, Ibaraki Prefecture, where the experiment was conducted.

Also, we consider that, as mentioned in the section on the input-output characteristics, the gain variations for SSPAs by measurement year are influenced by changes in the strength of receiving signals due to distortion of the large deployable antenna used for S-band transmission.

6.3 Amplitude-frequency characteristics

Figure 11 shows an example of the measurement results of the amplitude-frequency characteristics at the forward link (Fig.3). The horizontal axis represents the frequency, while the vertical axis represents the strength of receiving signals.

Figure 11 shows that no abnormal amplitude change was observed, indicating that the characteristics were good. Consequently, it was demonstrated that there was no degradation in the amplitude-frequency characteristics due to aging, indicating flat and good characteristics as amplitude-frequency characteristics of the transponder.

6.4 Spurious characteristics

Figure 12 shows an example of the measurement results of the spurious characteristics at the forward link (Fig. 3). The horizontal axis represents the frequency, while the vertical axis represents the strength of receiving signals.

As for the out-of-band spurious characteristics of ETS-VIII, the D/U value was more than 50 dB⁽⁴⁾ for the forward link (Fig. 3); however, the D/U value could not be accurately measured because of the increase in the noise floor due to the noise that the earth station received during the experiment. Therefore, we determined the value by whether there were unnecessary spurious emissions exceeding the noise floor.

Figure 12 shows that no unnecessary spurious emissions were observed, indicating that the spurious characteristics were good. It was demonstrated that there was no degradation in the spurious characteristics due to aging at the transponder of ETS-VIII, indicating good characteristics as a transponder.

6.5 Variable-gain characteristics

Figure 13 shows the measurement results of the variable-gain function of the S-band up-converter No.2 (S-TX2) at the forward link (Fig. 3). The horizontal axis represents the gain set value of the S-band up-converter, while the vertical axis represents the gain-variable amount for each set value (S-TX2 GAIN STS).

Figure 13 shows that there was almost no degradation in the characteristics, indicating that the characteristics are good. Also, the data coincide well with that of the initial

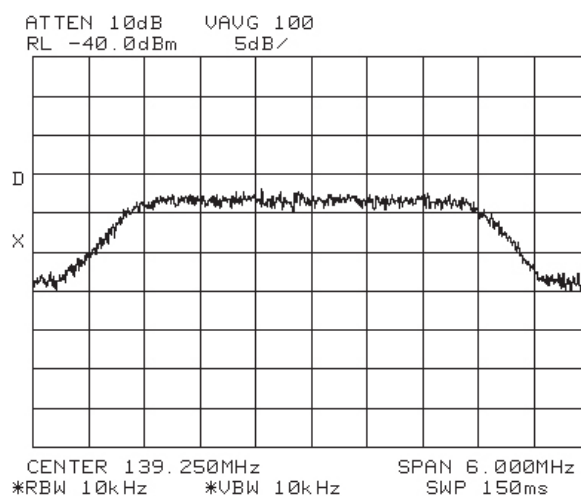


Fig. 11 Amplitude - frequency characteristics (an example of the forward link)

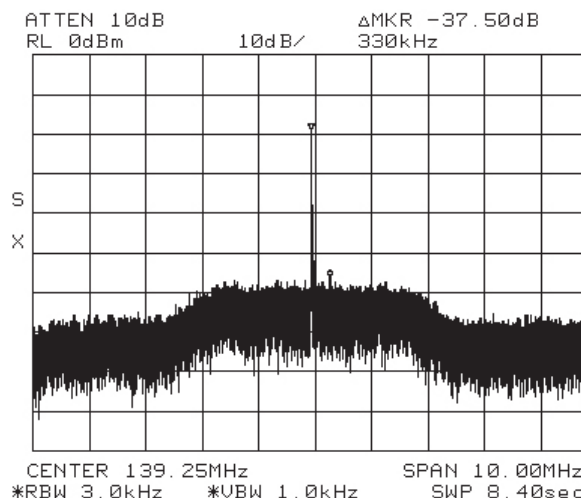


Fig. 12 Spurious characteristics (an example of the forward link)

performance evaluation experiment; therefore, it was demonstrated that the expected functions and performance of the gain-variable functions were maintained.

6.6 Frequency-variable characteristics

Figure 14 shows the measurement results of the frequency-variable function of the local oscillator (S-LO) for the S-band up-converter (S-TX) at the forward link (Fig.3). The horizontal axis represents the frequency set value of the S-band local oscillator (main system), while the vertical axis represents the frequency-variable amount at the same point in time.

Figure 14 shows that almost no degradation was observed in the characteristics, indicating that the characteristics were good. Also, the data coincide well with that of the initial performance evaluation experiment; therefore, it was found that the expected functions and performance were maintained.

Thus, it was identified that there was no aging degradation observed in the frequency-variable function of the local oscillator, and that the local oscillator was working as designed.

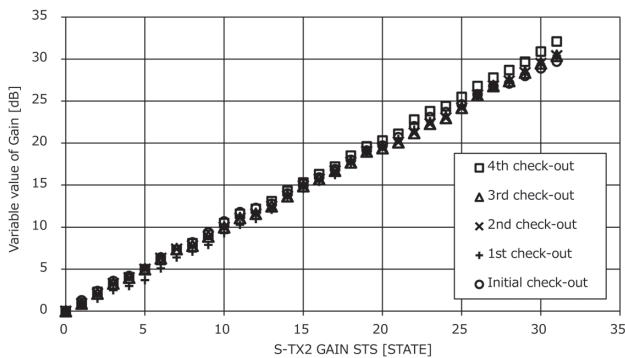


Fig. 13 Gain-variable characteristics (S-band up converter)

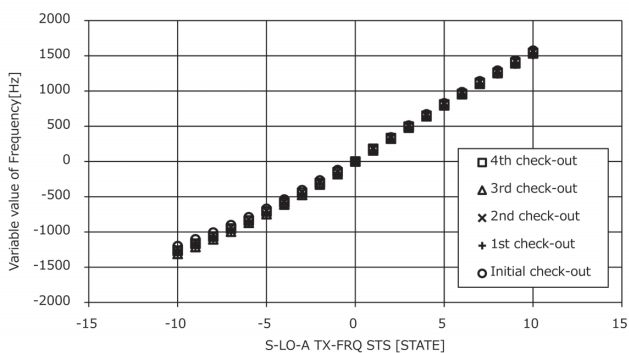


Fig. 14 Frequency-variable characteristics (S-band local oscillator)

7 Conclusion

The author has given an account of the evaluation of the characteristics and aging changes of transponders as the results of performance evaluation experiments of transponders, in which we measured the input-output characteristics, amplitude-frequency characteristics, spurious characteristics and frequency-variable characteristics during five years from the initial performance evaluation experiment (2007) to the fourth regular performance evaluation experiment (2012).

Since the experiment results were largely consistent, and there was no clear degradation observed in comparison with the data of the initial performance evaluation experiment, it was demonstrated that there were no significant changes to the performance and functions of transponders themselves, and that transponders maintained the expected performance. However, certain variations that were presumably caused by the distortions of LDRs were identified in the data obtained at the relay link that used the S-band large deployable antenna among the data such as those of the input-output characteristics or the transponder gain.

The technical achievements from ETS-VIII will be conducive to designing and manufacturing satellite onboard equipment in the future.

Acknowledgment

The author is deeply grateful to those concerned and those of related organizations who offered comments and cooperation in conducting this experiment.

References

- 1 S. Taira, "The mobile satellite communications and broadcasting system for the Engineering Test Satellite Eight (ETS-VIII)," IEICE General Conference, TB-1-3, pp. "SS-4" - "SS-5", March. 2003. (in Japanese)
- 2 S. Kozono, "Configuration for Mobile Communication satellite System and Broadcasting Satellite Systems," Journal of NICT Special Issue on the Engineering Test Satellite VIII, Vol. 50, Nos. 3/4, pp. 23-31, September/December, 2003. (in Japanese)
- 3 F. Kawasaki, Y. Kawakami, and M. Miyauchi, "Design of ETS-VIII on-board transponder," IEICE Society Conference, B-3-14, p. 178, Sept. 1998. (in Japanese)
- 4 H. Kohata and S. Hama, "Onboard Ka-band Feeder Link Communications Equipment," Journal of NICT Special Issue on the Engineering Test Satellite VIII, Vol. 50, Nos. 3/4, pp. 41-49, September/December, 2003. (in Japanese)
- 5 Y. Hashimoto, "S-band Frequency Converter," Journal of NICT Special Issue on the Engineering Test Satellite VIII, Vol. 50, Nos. 3/4, pp. 51-55, September/December, 2003. (in Japanese)
- 6 K. Ueno, "Configuration of the Feed System," Journal of NICT Special Issue

- on the Engineering Test Satellite VIII, Vol. 50, Nos. 3/4, pp. 57–66, September/December, 2003. (in Japanese)
- 7 H. Noda, K. Sano, and S. Hama, "High Accuracy Clock (HAC), " Journal of NICT Special Issue on the Engineering Test Satellite VIII, Vol. 50, Nos. 3/4, pp. 101–107, September/December, 2003. (in Japanese)
 - 8 S. Kozono, S. Taira, Y. Hashimoto, T. Ide, and S. Yamamoto, "Mobile Satellite Communications System for the ETS-VIII –Test of the Electrical Performance–," IEICE General Conference, B-3-12, p. 343, March. 2003. (in Japanese)
 - 9 S. Kozono, H. Watanabe, M. Satoh, S. Yamamoto, and S. Taira, "Initial performance of the transponder system for the ETS-VIII on the satellite orbit," IEICE Society Conference, BS-2-1, pp."S-12" – "S-13", Aug. 2007. (in Japanese)
 - 10 M. Satoh, T. Orikasa, and Y. Fujino, "Evaluation of Electrical Performance for Large-Scale Deployable Reflector Antenna Equipped with Engineering Test Satellite VIII on Orbit," IEICE Trans. Commun. (B), Vol. J94-B, No. 3, pp. 344–352, 2011.



Kazuyoshi KAWASAKI

Senior Researcher, Space Communication
Systems Laboratory, Wireless Network
Research Institute
Satellite Communication